$$t_{mn} = \begin{cases} \delta_{mn} \\ \varepsilon^{(o)}\xi_{n-m}(x)|_{x=0} \end{cases} \text{ and}$$

$$t_{mn} = \begin{cases} \delta_{mn} & \text{for TE modes} \\ \varepsilon^{(o)}\xi_{n-m}(x)|_{x=t_g} & \text{for TM modes} \end{cases} \quad (8)$$

where ξ_{n-m} is the $(n\text{-}m)$th coefficient of the Fourier series expansion of the inverse of permittivity, δ_{mn} the Dirac delta function and $\varepsilon^{(i)} = n^{(i)2}$ where $n^{(i)}$ is the refractive index of the ith layer. Moreover, $\mathbf{L}_0$ is a matrix with elements

$$l^0_{mn} = \begin{cases} jk^{(s)}_{xn}\delta_{mn} & \text{TE polarisation} \\ jk^{(s)}_{xn}\delta_{mn}\frac{\varepsilon^{(o)}}{\varepsilon^{(r)}} & \text{TM polarisation} \end{cases} \quad (9)$$

and $\mathbf{L}_g$ is a matrix with elements

$$l^{(g)}_{mn} = -jk^{(o)}_{xn}\delta_{mn} \quad (10)$$

The index m comes from the boundary conditions applications; it also denotes the harmonic order and for each n, m also ranges from $-\infty$ to $+\infty$.

Using Maxwell's equations in the PBG region we obtain a differential equation system to be solved using the boundary conditions of eqns. 6 and 7 and assuming k_{z0} is an unknown parameter. The numerical integration of the system has been carried out by a fifth-order Runge-Kutta-Fehlberg algorithm and the search for the complex eigenvalue k_{z0} has been performed using a polynomial form of Muller's routine. Having found k_{z0}, the other propagation constants, field amplitudes and phases and then, the power flow and reflection and transmission coefficients can be calculated.

For this purpose we have developed [2] a general model of transmittivity and reflectivity, accounting for any arbitrary number of field harmonics, where the field continuity conditions at interfaces (i.e. at $z = 0$ and $z = L$) enable ρ and τ to be determined, which are the field transmission and reflection coefficients, respectively. Thus the modal reflection coefficient $R_P = |\rho|^2$ and the modal transmission coefficient $T_P = |\tau|^2$ can be obtained.

The cover (substrate) radiation efficiency is simply given by the power density radiated in the cover (substrate) divided by the total radiated power density.

Table 1: Parameters of considered FWPBG structure

n_c	1
n_r	2
n_s	1.45
t_g [μm]	0.50
L [μm]	8.60
Λ [μm]	0.43

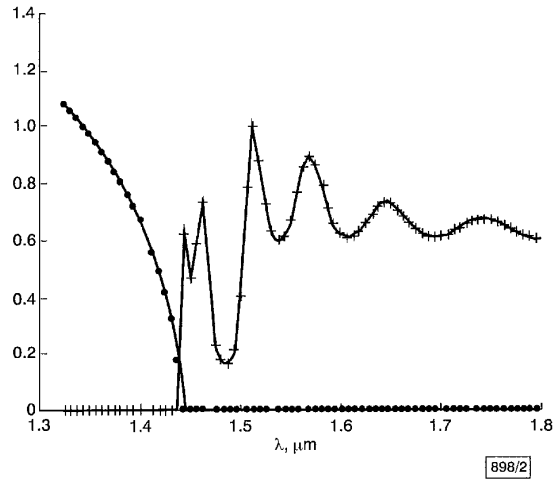

Fig. 2 *Transmittivity and radiation loss spectrum for simulated FWPBG*

—●— α (1/μm)
—+— transmittivity, T

The computer program in FORTRAN 77 language has been implemented on a 500 MHz PC; it performs all calculations to completely characterise the structure in a few seconds (~5). An analysis in correspondence of 100 operating wavelengths is completed in a few minutes (4–5).

Results: To validate our model we have compared our results with those calculated in [1] by using an exact vectorial model and the agreement is excellent, the maximum percentage relative difference being of 0.01% in the β_n calculation and 0.1% in the α calculation, for both TE and TM modes. The analysis was performed successfully for a structure etched down to the substrate with the parameters as listed in Table 1.

The transmission and radiation loss spectrum is shown in Fig. 2. A correspondence between the bandgap position (higher values of attenuation constant, α) and the transmittivity drop can be seen. Outside the bandgap, the transmittivity oscillates due to reflection to input and output section discontinuities.

Comparisons of results obtained using the bidirectional mode expansion and propagation (BEP) method show that the maximum percentage relative error on the gap calculation is < 0.01%.

The main advantage of the model is the absence of any *a priori* assumption and approximation, the speed and stability of the convergence, and the large amount of information and figures of merit that can be determined in a few seconds. An accurate determination of the bandgap position is allowed and structures with arbitrary profiles and finite length can be investigated. The real behaviour of PBG devices as perfect reflectors can be successfully predicted by our model which enables the designer to have a complete view on the physical and geometrical device features, and to draw up design rules for optimising of waveguide PBG device design easily and quickly.

31 March 2001
Electronics Letters Online No: 20010585
DOI: 10.1049/el:20010585

A. Giorgio, A.G. Perri and M.N. Armenise (*Politecnico di Bari, Dipartimento di Elettrotecnica ed Elettronica, via E. Orabona, 4, 70125 Bari, Italy*)

E-mail: perri@poliba.it

References

1 PENG, C.S., TAMIR, T., and BERTOM, H.L.: 'Theory of periodic dielectric waveguides', *IEEE Trans. Microw. Theory Tech.*, 1975, **MTT-23**, (1), pp. 123–133

2 GIORGIO, A., PERRI, A.G., and ARMENISE, M.N.: 'Very fast and accurate modelling of multilayer waveguiding photonic band-gap structures', to be published in *J. Lightwave Technol.*

Modes of Möbius resonator

J.M. Pond

The modes in a Möbius wire-loaded cavity resonator are discussed. In addition to the higher order Möbius modes, which occur at odd integer multiples of the fundamental mode resonant frequency, a set of modes, which occur at approximately even integer multiples of the fundamental Möbius resonant frequency, are discussed. These modes arise from the presence of the cavity wall and are related to even modes of a coupled line system.

Introduction: Dual-mode Möbius resonators which rely on a geometrical deformation of a transmission line to obtain a four-fold reduction in volume have been previously introduced [1, 2]. In the mathematical language of topology, these resonators are related to the study of non-orientable surfaces. Although traditionally referred to as one-sided surfaces, non-orientable surfaces are those for which the concept of left and right are globally nonsensical [3].

The Möbius strip is the prototypical non-orientable surface in that all non-orientable surfaces contain a Möbius strip. The Möbius strip possess the unique property that there is an apparent periodic alternation between left and right as the centre circle of a

Möbius strip is traversed. If a transmission line is projected onto a non-orientable surface with phasing required to sustain the electromagnetic oscillation along the path length associated with reversal of left and right, a resonant condition occurs with a volume reduction of a factor of four [1, 2].

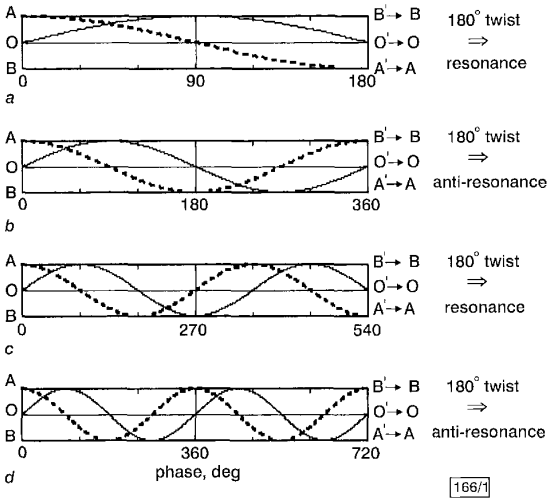

Fig. 1 *Illustration of conditions required for resonance of Möbius wire resonator*

Orthogonal modes satisfy resonance condition when centre circle length (O-O′) is odd integer multiple of λ/2, but are anti-resonant when centre circle length is even integer multiple of λ/2

Discussion: A convenient way of visualising the modes in such a resonator is to consider a twin conductor transmission line projected onto a Möbius strip. The conductor can be visualised as the edge of the Möbius strip and an electric field flux line can be considered as laying on the non-orientable surface. The Möbius strip can be formed from a rectangle by twisting one edge of the rectangle with respect to its opposite edge by 180° and joining these two edges. This twisting of the transmission line geometry by 180° results in a similar phase reversal of an electromagnetic field.

Fig. 1*a* illustrates the two fundamental orthogonal modes that can exist in a Möbius resonator. The electrical length of the transmission line projected onto the non-orientable surface is a half wavelength. Assuming that the centre circle (O-O′) of the Möbius strip formed in Fig. 1*a* is geometrically a circle (the term circle has a different meaning to topologists [3]), then the fundamental resonance occurs at $\pi d_o = \lambda/2$, where d_o is the radius. Due to the twist that exists in the transmission line, the resonator does not have a resonant condition at twice the fundamental frequency. This is illustrated in Fig. 1*b*, where it can be seen that an electrical length of 360°, combined with 180° of deformation, results in an anti-resonant condition. Similarly, we can see from Figs. 1*c* and *d* that resonant conditions will exist for odd-integer multiples of the fundamental but not for even-integer multiples of the fundamental. Specifically, resonance will exist when $\pi d_o = (2n + 1)\lambda/2$ (with n = 0, 1, 2, ...).

Fig. 2 *Möbius wire resonator and twin-loop wire resonator*

Mean diameters of both resonators were 1.94 cm
a Möbius resonator *b* Twin-loop resonator

Experiment: The twin-lead transmission line structures shown in Fig. 2 were fabricated and measured to demonstrate and compare the resonant behaviour of a regular twin-lead transmission line and a Möbius resonator. Both resonators were placed in a 2.54 cm diameter copper cavity (which, when empty, possessed a fundamental resonance at 9.04 GHz) which had two loop probes to weakly couple to the wire resonator. The measured transmission response of both resonators when weakly coupled is shown in Fig. 3. As expected the fundamental resonance of the Möbius resonator is at approximately half the fundamental resonance of the conventional twin lead (double loop) resonator. However, unlike the modes predicted by $\pi d_o = (2n + 1)\lambda/2$ (with n = 0, 1, 2, ...), it can be seen that resonances exist that nearly correspond with even-integer multiples of the fundamental frequency. These additional modes are not Möbius modes but, rather, result from placing the wire structure in a cavity.

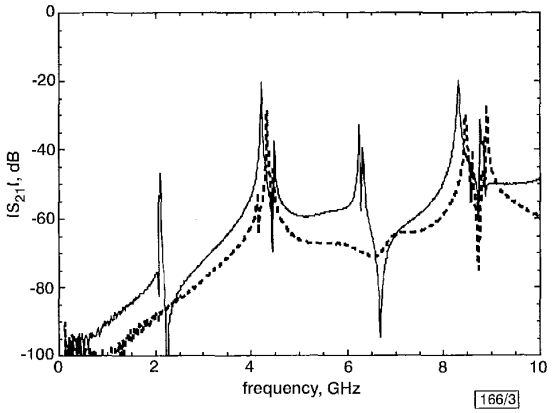

Fig. 3 *Measured transmission response of both resonators when placed in 2.54 cm diameter copper cavity*

——— Möbius resonator – – – – twin-loop resonator

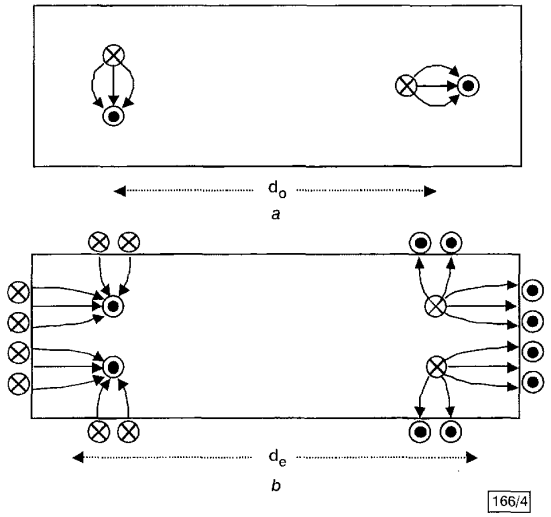

Fig. 4 *Currents and electric fields for Möbius and generalised even modes*

a Möbius modes *b* Generalised modes

Unlike in isolation, when inserted in a conducting cavity, locally (for a cross-section) there exists a coupled lined geometry with respect to the cavity wall which is at 'ground' potential. Fig. 4 illustrates the general differences in the current and electric field distribution of the two types of modes. The Möbius modes interact only minimally with the cavity walls since the currents in the two conductors are counter flowing. The other set of modes involves nearly equal currents in both wires flowing in the same direction and requires a counter flowing current in the cavity wall. These modes will occur when $\pi d_e = n\lambda$ (with n = 1, 2, 3, ...), where πd_e is the mean circumference of the transmission line defining this mode. This set of modes, which can be considered to be a set of even modes of the associated non-uniform coupled transmission

lines [4], does not exist except when the wire structure is inserted in a cavity. In the geometries measured $d_c \cong d_o$, and hence, the even modes appear at the approximately even integer multiples of the frequency of the fundamental Möbius resonance.

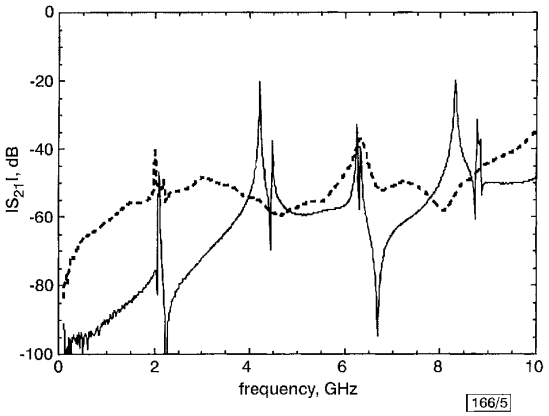

Fig. 5 *Comparison of resonances obtained by weakly coupling to Möbius wire resonator in 2.54 cm diameter copper cavity and on foam pedestal*

– – – Möbius wire – – – – foam pedestal

This explanation was confirmed by measuring the response of the Möbius wire resonator when placed on an electromagnetically transparent foam pedestal. The Möbius wire resonator was illuminated and the forward-scattered signal was measured. The orientation of the resonator was varied with respect to both the illumination signal as well as the receiver to ensure that the lack of a response at frequencies near the even integer multiples of the dominant Möbius mode frequency was not caused by a fortuitous geometry. A typical response is shown in Fig. 5, where, for comparison, the response measured in the cavity is repeated. Clearly, the modes at the even-integer multiples of the fundamental Möbius mode frequency do not exist without the presence of the cavity walls to support the counter-flowing current.

Conclusions: The modes of a Möbius resonator have been discussed. The higher order Möbius modes are shown to exist only at odd-integer multiples of the fundamental mode. When realised as a wire-loaded cavity resonator it was shown that the additional modes that occur at approximately even-integer multiples of the fundamental mode are not Möbius modes, but rather are associated with generalised even modes where current flow in the cavity wall is required for resonance. Suppression of the generalised even modes will facilitate the design and fabrication of Möbius filters with superior out-of-band rejection.

Acknowledgment: The author would like to thank the United States Office of Naval Research for supporting this work.

10 April 2001
Electronics Letters Online No: 20010573
DOI: 10.1049/el:20010573

J.M. Pond (*Microwave Technology Branch, 4555 Overlook Avenue, S.W., Naval Research Laboratory, Washington, DC 20375, USA*)

E-mail: pond@chrisco.nrl.navy.mil

References

1 POND, J.M.: 'Möbius filters and resonators'. 2000 IEEE MTT-S, Int. Microwave Symp. Dig., June 2000, Vol. 3, pp. 1653–1656

2 POND, J.M.: 'Möbius dual-mode resonators and bandpass filters', *IEEE Trans. Microw. Theory Tech.*, 2000, **MTT-48**, (12), pp. 2465–2471

3 CARTER, J.S.: 'How surfaces intersect in space: an introduction to topology' (World Scientific Publishing Co. Pte. Ltd., Singapore, 1995), 2nd edn.

4 ADAIR, J.E., and HADDAD, G.I.: 'Coupled-mode analysis of nonuniform coupled transmission lines', *IEEE Trans. Microw. Theory Tech.*, 1969, **MTT-17**, (10), pp. 746–752

Multilayer elliptic filter

R.W. Jackson and Hsiao-Chun Hsu

A compact configuration for a four pole elliptic filter is described. This filter stacks quarter wave resonators in a novel manner that is particularly suitable for multilayer ceramic packaging. A design procedure is discussed. Simulations and measurements of a prototype filter are presented.

Introduction: Elliptic filters are often used in mobile communications transceivers because their transmission zeros can be used to limit interference to or from adjacent channels, e.g. in PCS applications. Since several such filters may be used in a single mobile radio, the most useful filter realisations must be as small as possible while still retaining good low loss characteristics. Because of its stacked nature, the filter we describe in this Letter is particularly compact, being half the size of an unstacked version. Its construction is also compatible with common low cost planar ceramic fabrication processes.

In contrast to fully planar microstrip filters such as the microstrip square open loop filter [1], the stacked configuration described herein allows more space for each resonator and therefore a higher Q. However, the stacked structure does not as yet include the cross coupling effects that make [1] so interesting.

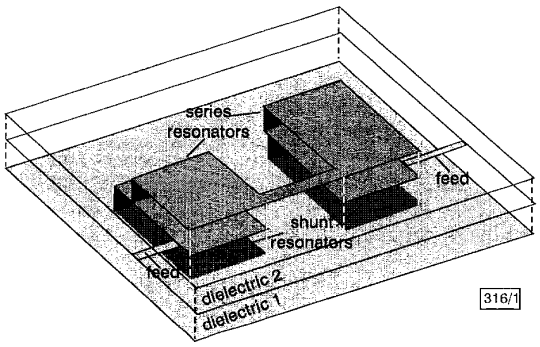

Fig. 1 *Illustration of elliptic filter with stacked resonators*

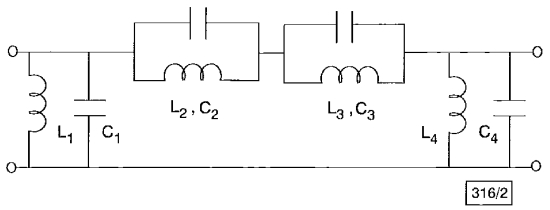

Fig. 2 *Elliptic filter circuit topology*

Fig. 1 illustrates the multilayer elliptic filter structure. Two layers of dielectric are shown sitting upon a conducting ground plane. There are four, quarter wavelength short circuit transmission line resonators (SCTL). The purpose of these resonators is best explained by referring to the classic elliptic filter circuit shown in Fig. 2. The two SCTL resonators just above the ground plane in Fig. 1 are the shunt resonators shown in Fig. 2. The bottom conductor of the series SCTLs is located between the dielectric layers and coincides with the top conductor of the shunt SCTLs. The top conductors of the series SCTLs are on the upper surface of the top dielectric layer. A transmission line on that surface connects one shunt-series pair to the other. Via trenches at the ends of the resonators we short circuit the top plate to the middle plate and the middle plate to the ground plane. Feed lines are located on the top surface of the lower dielectric layer and connect to the upper conductor of the shunt SCTLs.

Design procedure: A mix of electromagnetic simulation and circuit modelling is used in the design of this filter. Standard tables are used to establish component values for the lumped element prototype in Fig. 2. The length of each physical resonator is initially set to be one-quarter wavelength at the resonant frequency of the cor-